Applied Physics Letters ARTICLE scitation.org/journal/apl

Identifying the dominant carrier of CdSe-based blue quantum dot light-emitting diode

Cite as: Appl. Phys. Lett. **122**, 113501 (2023); doi: 10.1063/5.0142735
Submitted: 16 January 2023 · Accepted: 24 February 2023 ·
Published Online: 13 March 2023

Xiangwei Qu,[1,2] Guohong Xiang,[1,2] Jingrui Ma,[1,2] Pai Liu,[1,2] Aung Ko Ko Kyaw,[1,2] Kai Wang,[1,2] and Xiao Wei Sun[1,2,a)]

AFFILIATIONS

[1]Institute of Nanoscience and Applications, and Department of Electrical and Electronic Engineering, Southern University of Science and Technology, Shenzhen 518055, China

[2]Key Laboratory of Energy Conversion and Storage Technologies (Southern University of Science and Technology), Ministry of Education, Guangdong University Key Laboratory for Advanced Quantum Dot Displays and Lighting, Guangdong-Hong Kong-Macao Joint Laboratory for Photonic-Thermal-Electrical Energy Materials and Devices, and Shenzhen Key Laboratory for Advanced Quantum Dot Displays and Lighting, Southern University of Science and Technology, Shenzhen 518055, China

[a)]**Author to whom correspondence should be addressed:** sunxw@sustech.edu.cn

ABSTRACT

Unlike red and green quantum dot light-emitting diodes (QLEDs), it is not clear whether a blue QLED is an electron-dominated device. In this work, we identify that electron is over-injected in blue QLEDs by impedance spectroscopy. By analyzing the capacitance–voltage characteristics of the single-carrier devices, we find that the built-in voltage of the electron-only device is smaller than that of the hole-only device. Therefore, electron injection is more efficient than hole injection in blue QLEDs. To support our arguments, we employ a red QD as a fluorescent sensor to spatially investigate the exciton recombination zone of a blue QLED. Consequently, we observe that the exciton recombination zone of the blue QLED is close to the hole transport layer, and it shifts toward an electron transport layer with the increase in the applied bias. Our work provides a practical method for identifying the excess carrier in blue QLEDs, and it could be applied to other types of QLEDs.

Quantum dot light-emitting diodes (QLEDs) are becoming a promising flat panel display technology owing to its size tunable emission wavelength, narrow linewidth, high performance, and low cost fabrication process.[1–7] Since its emergence in 1994,[1] extensive efforts have been continuously devoted to improving its electroluminescence (EL) efficiency and operational lifetime. For instance, the maximum external quantum efficiency (EQE) of state-of-the-art red, green, and blue QLEDs has reached 30.9%, 28.7%, and 21.9%, respectively.[4,5] The operational lifetime T_{95} of red and green QLEDs is 7668 and 7200 h[4,7] (at the initial luminance of 1000 cd/m^2). However, the operational lifetime of blue QLEDs is just 57 h,[4] which needs to be improved to meet the standard of display application.

Apart from the operational lifetime, there still remain some basic issues to be solved in blue QLEDs. For example, in red and green QLEDs, electron injection is more efficient compared to hole injection.[2–6] However, it is not clear whether the blue QLED is an electron-dominated device. To identify the excess carrier, a general method is to compare the current density of the single-carrier devices.[8,9] However, the widely employed electron transport layer (ETL) in QLEDs is ZnO nanoparticles, which is an inorganic material with high electron mobility. However, the hole transport layer (HTL), either poly((9,9-dioctylfluorenyl-2,7-diyl)-co-(4,4′-(N-(4-sec-butylphenyl) diphenylamine))) (TFB) or poly(9-vinlycarbazole) (PVK), is an organic semiconductor with lower hole mobility.[10] The current density of an electron-only device is usually much higher than that of a hole-only device. Therefore, other methods are needed to facilitate the identification of the excess carrier. For instance, Deng *et al.* observed the electron leakage in blue QLEDs, which proved the electron over-injection in blue QLEDs[4] is significant. To improve the performance of blue QLEDs, they employed poly((9,9-dioctylfluorenyl-2,7-diyl)-alt-(9–(2-ethylhexyl)-carbazole-3,6-diyl)) (PF8Cz) as the HTL to suppress the electron leakage. However, some works showed the opposite. Chen *et al.* concluded that hole injection in blue QLEDs is faster than electron injection by the electro-absorption measurement;[11] they also observed electron accumulation at the QD–ZnO interface, which caused the lifetime degradation of blue QLEDs. Therefore, some debates still exist about the excess carrier of blue QLEDs.

Impedance spectroscopy is a useful technique for solar cell and organic light-emitting diode (OLED)[12–14] characterization, and it was also applied in QLEDs recently. Blauth *et.al.* observed negative

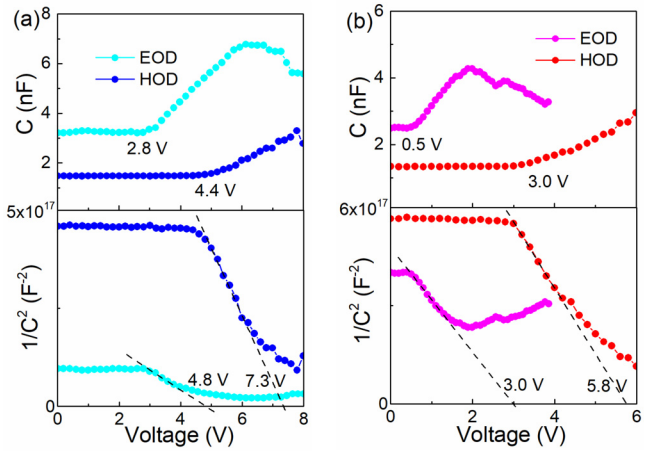

FIG. 1. Capacitance–voltage and $1/C^2$-voltage characteristics of (a) blue and (b) red single-carrier devices.

capacitance of QLEDs at a low frequency owing to the non-luminescent recombination.[15] Qian *et.al.* monitored the QLED degradation process and studied its degradation mechanism by impedance spectroscopy.[6,11] In our previous work, we employed it to identify the surface charge of quantum dots and investigated its impact on the charge dynamics of QLEDs.[16] In addition to these findings, more relevant data can be analyzed using this method. In this work, we employed impedance spectroscopy to study charge injection in blue single-carrier devices. With the Mott–Schottky analysis of single-carrier devices, the built-in potential of the electron-only device is found to be 5.0 V, while it is 7.4 V for the hole-only device. Therefore, the blue QLED is an electron-dominated device. To support our argument, a red QD is used as a fluorescent sensor to investigate the exciton recombination zone of a blue QLED. Consequently, we observed that the exciton recombination zone of the blue QLED is close to the HTL, and it migrates toward the ETL as the applied bias increases. Our method can be applied to other types of QLEDs to identify the excess carriers. It provides a guide to improve the performance of blue QLEDs.

Under strong Coulomb interaction, electron and hole injections in QLEDs are affected by each other.[14,21] It is difficult to identify the dominating carrier in a dual-carrier injected blue QLED. Therefore, we study the charge injection in a single-carrier blue QLED. Lee *et al.* have identified that hole injection is more efficient than electron injection in OLEDs by single-carrier devices,[17] indicating that it is a practical method. The electron-only device (EOD) is fabricated with the structure of ITO/ZnMgO/QD/ZnMgO/Al, and the hole-only device (HOD) is structured as ITO/PEDOT:PSS/TFB/QD/TCTA/NPB/HATCN/Al. As a comparison, the red single-carrier devices are also fabricated. Figure 1(a) shows the capacitance–voltage characteristics of blue single-carrier devices. At the low applied bias, the capacitance of a blue EOD is contributed by its geometric capacitance (3.2 nF) and remains unchanged, implying that no charge is injected into the device. As the applied bias increases to 2.8 V, the capacitance starts to increase, which suggests that electrons are injected and accumulated in the device. As for the blue HOD, hole injection starts at 4.4 V. Therefore, electron injection requires less bias, i.e., it is more efficient than hole injection. In such a case, the current density of the blue EOD is much larger than that of the blue HOD (Fig. S1). For instance, at the applied bias of 6 V, the current density of the blue EOD is 7.43 mA/cm^2, while it is only 0.56 mA/cm^2 for the blue HOD. For red single-carrier devices, the electron is injected at 0.5 V, while hole injection starts at 3.0 V. Therefore, the charge injection of blue single-carrier devices is similar to the red ones.

On the other hand, the built-in potentials of blue and red single-carrier devices can be estimated by Mott–Schottky equation. The Mott–Schottky analysis is a well-known method to determine built-in potentials based on the property of a PN junction, which has been already applied in solar cells, OLEDs, and QLEDs recently.[3,13,18] The built-in voltage of single-carrier devices is estimated from the slope and intercept of the C^{-2} −V plot, based on the following Mott–Schottky equation:[18]

$$\frac{1}{C^2} = \frac{2}{q\varepsilon A^2 N_A}(V_{bi} - V),$$

where C is the device capacitance, q is the elementary charge, ε is the dielectric constant, A is the active area of the single-carrier devices, N_A is the total doping density, V_{bi} is the built-in voltage, and V is the applied voltage. As shown in Fig. 1(a), the built-in voltage of the blue EOD is 4.8 V, while it is 7.3 V for the blue HOD, indicating the electron injection barrier is relatively small in the blue QLED. For the red

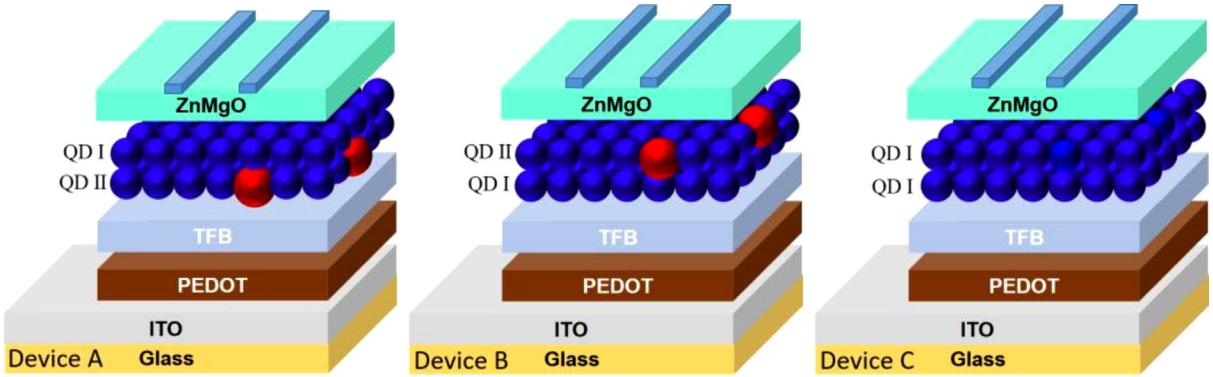

FIG. 2. Device structure diagrams of device A, device B, and device C.

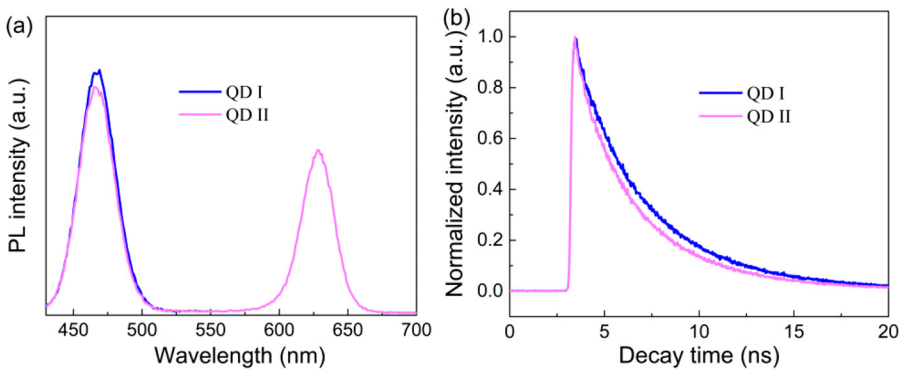

FIG. 3. (a) PL and (b) TRPL characteristics of QD I and QD II films.

EOD, the built-in voltage is 3.0 V for electrons, which is smaller than that of the hole in the red HOD (5.8 V). Therefore, the blue QLED is an electron-dominated device, similar to red ones. The efficient electron injection of blue QLED comes from the outstanding electron transport and injection ability of ZnMgO nanoparticles; once we employ 2,2″,2‴-(1,3,5-Benzinetriyl)-tris(1-phenyl-1-H-benzimidazole) (TPBi) as an ETL in the blue EOD, the built-in voltage of the blue EOD is dramatically increased to 12.7 V (Fig. S2), which is even higher than that of a blue HOD. Therefore, holes are the excess carrier in a TPBi-based blue QLED.[19] According to the impedance spectroscopy result of the single-carrier devices, ZnMgO nanoparticles enable efficient electron injection in blue QLEDs, which determines the blue QLED as an electron-dominated device.

To support our arguments, a red QD is further employed as a fluorescent sensor to investigate the exciton recombination zone of the blue QLED. The fluorescent probe method is widely employed to detect the exciton recombination zone in an OLED device.[20,21] A fluorescent probe layer can be placed at any position in an OLED device, and exciton recombination zone can be detected according to the emission of the fluorescent probe. We fabricated three types of QLED devices with a structure of ITO/PEDOT:PSS/TFB/QD/ZnMgO/Al, where ITO, PEDOT:PSS, TFB, QD, ZnMgO, and Al act as anode, hole

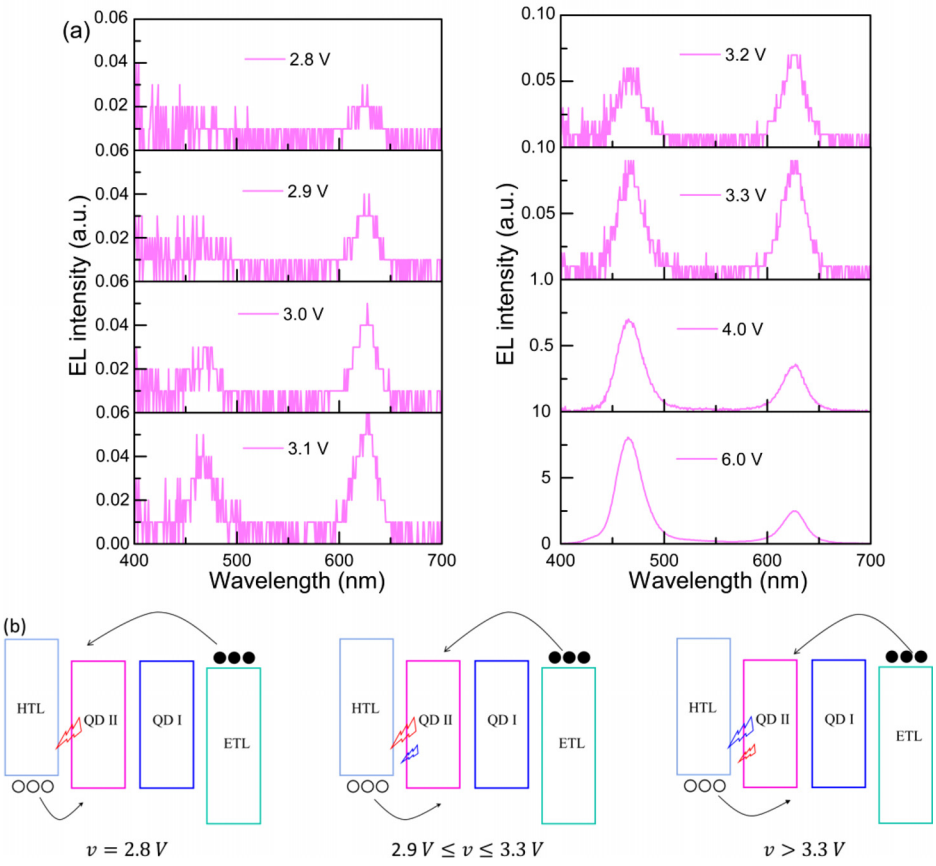

FIG. 4. (a) Varied EL spectra of device A and (b) exciton recombination center migration of device A.

injection layer, HTL, emission layer, ETL, and cathode, respectively. As illustrated in Fig. 2, device A contains a double QD layer, where the QD I layer is on top of the QD II layer. Herein, the QD I layer is a pure blue QD layer, and the QD II layer is a 3% red QD mixed blue QD layer (Fig. S3) with the red QD as a fluorescent sensor. QD I and QD II layers are cross-linked by a bifunctional ligand 1,8-diaminooctane.[22,23] Device B owns the same device structure, but the QD II layer is on top of the QD I layer. Device C is the control blue QLED, including the double QD I layer. As shown in Fig. S4, devices A, B, and C show the nearly same current density–voltage characteristics. Therefore, the emission of the red fluorescent sensor can reflect the exciton recombination zone in blue QLEDs.

Next, we have to identify the origin of red emission in a blue QLED, i.e., it is mainly from a Förster resonant energy transfer (FRET) process or direct charge injection. The FRET process happens between closely packed donors and acceptors, which requires a spectrum overlap of a donor and an acceptor.[24] As shown in Fig. S5, the PL emission of a blue QD can be absorbed by a red QD, which provides a probability of the FRET process in the QD II layer. To depict the FRET process between red and blue QDs in detail, we examine the PL and TRPL characteristics of the QD I and QD II films. As shown in Fig. 3(a), the PL spectrum of blue and red QDs peak at 464 and 628 nm, respectively. When the blue QD is mixed with 3% red QD, the PL intensity of blue emission has only a little drop, which indicates a small energy loss. The red emission is strong enough, which may come from a high quantum yield of red QD. Figure 3(b) shows that the TRPL kinetics (detected at 464 nm) of the QD II film is slightly shorter than that of the QD I film, which implies that the FRET process has little effect on the exciton lifetime of the QD II film. Specifically, the FRET efficiency is calculated as[24]

$$\eta = 1 - \frac{\tau_{RB}}{\tau_B},$$

where τ_{RB} is the exciton lifetime of the QD II film and τ_B is the exciton lifetime of the QD I film. According to the fitting data in Table S1, the exciton lifetime of QD II and QD I films is estimated to be 3.26 and 3.81 ns, respectively. Therefore, the FRET efficiency is estimated to be 14.4%. With a low mixing ratio of the QD II film, the FRET process is difficult to occur because of the long distance between the red QD and blue QD.[24] Consequently, the red emission in blue QLED is mainly from direct charge injection.

The varied EL spectrum of device A is shown in Fig. 4(a), we only observe a red emission in the EL spectrum at an applied bias of 2.8 V, which indicates that exciton is first formed in the QD II layer. Therefore, the exciton recombination zone is close to HTL, which is illustrated in Fig. 4(b). As the applied bias rises, blue emission appears in the EL spectrum, but its emission intensity is still lower than that of the red emission until 3.3 V. Within this voltage range, the red emission is dominating in the EL spectrum. However, the intensity of the blue emission with respect to the red emission is gradually increasing, suggesting that the exciton recombination center is migrating toward ETL. With further increase in the applied bias, blue emission is gradually dominating in the EL spectrum, the intensity of red emission with respect to blue emission is dropped from 1 to 31% when the voltage is increased from 3.3 to 6.0 V, indicating that the exciton recombination zone is gradually moving toward ETL. In this case, the proportion of blue emission in the QD I layer is increasing continuously, thereby resulting in the relative intensity drop of the red emission. As for device B, the QD II layer is on top of the QD I layer, and the blue emission is always dominating in the EL spectrum (Fig. S8), indicating that exciton recombination center is located in the QD I layer, which is

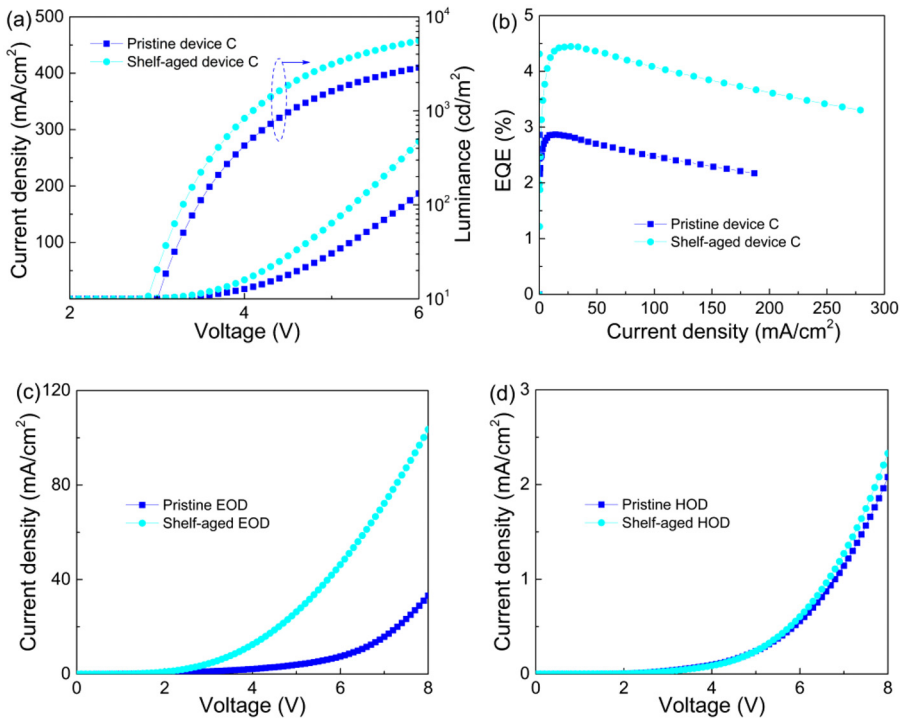

FIG. 5. (a) Current density–luminance–voltage characteristics and (b) EQE–current density characteristics of the pristine and shelf-aged device C, and current density–voltage characteristics of (c) pristine and shelf-aged EODs and (d) pristine and shelf-aged HODs.

consistent with the EL spectrum of device A. Therefore, the exciton recombination zone of the blue QLED is close to the HTL, which proves that the blue QLED is an electron-dominated device.

Although the blue QLED is an electron-dominated device, we suggest improving the performance of blue QLEDs by facilitating electron injection. As shown in Figs. 5(a) and 5(b), the current density, luminance, and EQE of blue QLEDs are improved simultaneously after several days of shelf aging. For instance, the current density of device C at 6 V is increased from 186 to 279 mA/cm^2 with shelf aging, and the max EQE of device C is increased from 2.86% to 4.45%. Compared to the current density of the pristine and shelf-aged single-carrier devices [Figs. 5(c) and 5(d)], the current density rise of blue QLEDs is mainly caused by the enhanced electron current. Therefore, blue QLEDs exhibit higher performance with improved electron injection. Actually, Deng *et al.* provided an interpretation that red QLEDs showed high performance with excess electron injection.[25] First, an electron was injected in the quantum dot layer, which made the quantum dot negatively charged; then, the negatively charged quantum dots would attract hole injection and repulse additional electron injection. After hole injection, an additional electron would be injected into the neutral-charged quantum dot. The self-regulated charge injection process makes a charge balance in red QLEDs. Therefore, it is reasonable to improve the performance of blue QLEDs by facilitating electron injection. Based on this strategy, various methods are employed to improve blue QLEDs,[26–28] because improved electron injection induces more efficient hole injection, which in turn enables highly efficient and stable blue QLED.

To summarize, we identified that blue QLEDs are an electron-dominated devices. According to the capacitance–voltage characteristics of the blue single-carrier devices, the blue HOD showed a larger built-in voltage than that of the blue EOD, which indicates that the electron injection barrier is relatively small. Therefore, electron injection is more efficient than hole injection in the blue QLED. In addition, we observed the exciton recombination zone is close to the HTL, evidenced by a red QD fluorescent probe. Despite the efficient electron injection, we suggest improving blue QLEDs by facilitating electron injection, because it would induce efficient hole injection in turn. Our work develops a practical method to study charge injection in blue QLEDs, and it may be applied to identify the excess carrier in other types of QLEDs.

See the supplementary material for the details of the experimental section, current density–voltage characteristics of single-carrier devices, impedance spectroscopy of TPBi-based single-carrier devices, diagram of the QD layer, current density–voltage characteristics of the blue QLED, absorption and PL spectra of QDs, PL spectra of pure red and blue QDs, PL, and TRPL spectra of devices A and B, varied EL spectra of device B, and shelf-aged devices A and B, and TRPL fitted data of QD.

This work was supported by the National Key Research and Development Program of China (Nos. 2021YFB3602703, 2022YFB3606504, and 2022YFB3602903), National Natural Science Foundation of China (No. 62122034), Guangdong University Key Laboratory for Advanced Quantum Dot Displays and Lighting (No. 2017KSYS007), and Shenzhen Key Laboratory for Advanced Quantum Dot Displays and Lighting (No. ZDSYS201707281632549).

AUTHOR DECLARATIONS

Conflict of Interest

The authors have no conflicts to disclose.

Author Contributions

Xiangwei Qu: Conceptualization (lead); Data curation (lead); Investigation (lead); Methodology (lead); Writing – original draft (lead). **Guohong Xiang:** Investigation (supporting); Methodology (supporting). **Jingrui Ma:** Investigation (supporting); Methodology (supporting). **Pai Liu:** Supervision (equal). **Aung Ko Ko Kyaw:** Supervision (equal). **Kai Wang:** Supervision (equal). **Xiao Wei Sun:** Project administration (lead); Supervision (lead); Writing – review & editing (lead).

DATA AVAILABILITY

The data that support the findings of this study are available from the corresponding author upon reasonable request.

REFERENCES

[1]V. L. Colvin, M. C. Schlamp, and A. P. Alivisatos, Nature **370**, 354 (1994).
[2]X. Dai, Z. Zhang, Y. Jin, Y. Niu, H. Cao, X. Liang, L. Chen, J. Wang, and X. Peng, Nature **515**(7525), 96–99 (2014).
[3]T. Kim, K. H. Kim, S. Kim, S. M. Choi, H. Jang, H. K. Seo, H. Lee, D. Y. Chung, and E. Jang, Nature **586**(7829), 385–389 (2020).
[4]Y. Deng, F. Peng, Y. Lu, X. Zhu, W. Jin, J. Qiu, J. Dong, Y. Hao, D. Di, Y. Gao, T. Sun, M. Zhang, F. Liu, L. Wang, L. Ying, F. Huang, and Y. Jin, Nat. Photonics **16**(7), 505–511 (2022).
[5]J. Song, O. Wang, H. Shen, Q. Lin, Z. Li, L. Wang, X. Zhang, and L. S. Li, Adv. Funct. Mater. **29**(33), 1808377 (2019).
[6]W. Cao, C. Xiang, Y. Yang, Q. Chen, L. Chen, X. Yan, and L. Qian, Nat. Commun. **9**(1), 2608 (2018).
[7]D. Liu, S. Cao, S. Wang, H. Wang, W. Dai, B. Zou, J. Zhao, and Y. Wang, J. Phys. Chem. Lett. **11**(8), 3111–3115 (2020).
[8]Q. Lin, L. Wang, Z. Li, H. Shen, L. Guo, Y. Kuang, H. Wang, and L. S. Li, ACS Photonics **5**(3), 939–946 (2018).
[9]L. Wang, T. Chen, Q. Lin, H. Shen, A. Wang, H. Wang, C. Li, and L. S. Li, Org. Electron. **37**, 280–286 (2016).
[10]H. Shen, Q. Lin, W. Cao, C. Yang, N. T. Shewmon, H. Wang, J. Niu, L. S. Li, and J. Xue, Nanoscale **9**(36), 13583–13591 (2017).
[11]S. Chen, W. Cao, T. Liu, S. W. Tsang, Y. Yang, X. Yan, and L. Qian, Nat. Commun. **10**(1), 765 (2019).
[12]I. D. Parker, J. Appl. Phys. **75**(3), 1656–1666 (1994).
[13]J.-M. Kim, C.-H. Lee, and J.-J. Kim, Appl. Phys. Lett. **111**(20), 203301 (2017).
[14]J. C. Nolasco, A. Sánchez-Díaz, R. Cabré, J. Ferré-Borrull, L. F. Marsal, E. Palomares, and J. Pallarès, Appl. Phys. Lett. **97**(1), 013305 (2010).
[15]C. Blauth, P. Mulvaney, and T. Hirai, J. Appl. Phys. **125**(19), 195501 (2019).
[16]Z. Wu, P. Liu, X. Qu, J. Ma, W. Liu, B. Xu, K. Wang, and X. W. Sun, Adv. Opt. Mater. **9**(17), 2100389 (2021).
[17]J. Lee, K.-J. Lee, M-k Kim, J-s Kim, C-k Yoo, H.-Y. Oh, S. Yoon, C.-D. Kim, and Y.-K. Hwang, in *SID Symposium Digest of Technical Papers* (Blackwell Publishing Ltd., Oxford, 2011), Vol. 42, pp. 1002–1005.
[18]B. Ray, A. G. Baradwaj, B. W. Boudouris, and M. A. Alam, J. Phys. Chem. C **118**(31), 17461–17466 (2014).
[19]X. Huang, H. Zhang, D. Xu, F. Wen, and S. Chen, ACS Appl. Mater. Interfaces **9**(33), 27809–27816 (2017).
[20]C. Weichsel, L. Burtone, S. Reineke, S. I. Hintschich, M. C. Gather, K. Leo, and B. Lüssem, Phys. Rev. B **86**(7), 075204 (2012).
[21]S. Ye, Y. Wang, R. Guo, Q. Zhang, X. Lv, Y. Duan, P. Leng, S. Sun, and L. Wang, Chem. Eng. J. **393**, 124694 (2020).
[22]O. V. Kozlov, Y.-S. Park, J. Roh, I. Fedin, T. Nakotte, and V. I. Klimov, Science **365**, 672–675 (2019).
[23]J. Roh, Y. S. Park, J. Lim, and V. I. Klimov, Nat. Commun. **11**(1), 271 (2020).

[24]Z. Qin, Q. Su, and S. Chen, Adv. Opt. Mater. **11**(4), 2022451 (2022).
[25]Y. Deng, X. Lin, W. Fang, D. Di, L. Wang, R. H. Friend, X. Peng, and Y. Jin, Nat. Commun. **11**(1), 2309 (2020).
[26]X. Qu, N. Zhang, R. Cai, B. Kang, S. Chen, B. Xu, K. Wang, and X. W. Sun, Appl. Phys. Lett. **114**(7), 071101 (2019).
[27]Z. Zhong, J. Zou, C. Jiang, L. Lan, C. Song, Z. He, L. Mu, L. Wang, J. Wang, J. Peng, and Y. Cao, Org. Electron. **58**, 245–249 (2018).
[28]L. Wang, J. Lin, Y. Hu, X. Guo, Y. Lv, Z. Tang, J. Zhao, Y. Fan, N. Zhang, Y. Wang, and X. Liu, ACS Appl. Mater. Interfaces **9**(44), 38755–38760 (2017).